An Evaluation of Topographic Correction Methods for Landsat Images

Author: Weihang Li

Abstract

Topography has a strong impact on earth remote sensing. The inclination of earth surface and vegetation will both affect the irradiance and the bidirectional reflectance distribution function (BRDF). In order to get correct reflectance and surface property data, it is importance to reduce or to eliminate the effect caused by geographical conditions. Over the years, methods have been developed to achieve this goal, these methods include the Minnaert correction method, the C-correction method, Lambert cosine correction method, sun-canopy-sensor method and physics-based method. In this paper, c-correction (CC) method, sun-canopy-sensor (SCS) method and the physics based BRDF method are introduced. CC and SCS methods are evaluated cooperating with digital Surface Model (DSM) to the Landsat 8 data at Chittenden Peak located in California, United States. Visual assessments show that after the imaging processing, all three algorithms reduced some amount of topographic effect and detected some shadowed surface. Each method show advantage in outcome for different sensing conditions, but both methods generally reduced the shaded pixels by around 70 presents after the image processing.

1. Introduction

Earth surface monitoring is an important application of satellite remote sensing. Monitoring the surface changes of earth can give us important information regarding land degradation and dynamic surface water extent. Gully erosion is a nature process occurring along stream channels where landscape collapse caused by flood impact or rainwater run-down (Ireland et al., 1939: 39). Development of gully erosion can cause destruction of infrastructure, agriculture land reduction and vegetation degradation (Tricart and Cailleux, 1972: 200). Monitoring gully erosion is an important indicator for predicting and governing erosion. Satellite remote sensing is an efficient way to monitor the erosion progress in large time scale (bell.A, 1987).

Gully erosion often happens in mountainous area and create a steep terrain near the riverbank which create difficulties in detection for optical satellite imaging through irradiance and BRDF effects (Dymond et al., 2001; Gu & Gillespie, 1998). The angle between the sun and the riverbank can largely affect the image since the side facing the sun would be brighter and the side facing away from the sun would be darker or shaded ((Iqbal, 1983, Chapters 10,11). Figure 1 is a simple diagram that illustrate the effect. In addition, surfaces reflection might also be affected by the land cover structure and the satellite azimuth angle (Li, F., 2012). Thus, topographic correction is necessary before further data process (Liang S., 2004).

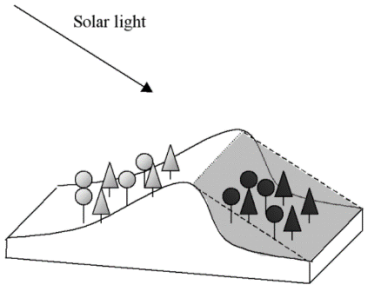

Fig. 1 steep terrain effect reflectance (Riaño, 2003)

Many models have been developed to correct the Landsat data (Li & Strahler, 1985; Schaaf, C, 2002; Vermote, E, 1997). These models have included algorisms for flat exposure surface, forest covered surface and inclining mountain surface. “C-correction” method is widely used to relate the observed radiance and the cosine of the incident angle (Richter, R.,1997). “C-correction” method uses a known reflectance at the reference area to derive a spatial map of the optical depth (Kaufman and Sendra 1988). Four radiometric correction (e.g., Meyer et al., 1993) is a statistic-empirical improvement of the “C-correction” on the rugged terrain. “Sun-Canopy-Sensor” method uses the position of the tree and the amount of

shadowing cast by the tree canopy to determine the inclination of the slope (Gu and Gillespie, 1998). "Physic-based" correction method is developed based on the physical~~ly~~ properties of the surface reflection and atmospheric correction (Li, F., 2012). Various models have been developed to perform topographic corrections, however, there isn't a universal method that can be drawn from existing methods since none of the existing methods transcend other methods by a considerable amount in all conditions. (Richter, 2009; Riaño 2003). Several authors have concluded that to achieve best correction results different method should be evaluated for individual locations and weather conditions.

Many satellite sensors have been launched for earth surface monitoring. Among them, Landsat is most widely used due to its publicity and the long-time span of continuity of data. Landsat-1 which is launched in 1972 is the first satellite that has been used in soil erosion detection through earth surface monitoring and Landsat-7,8 are still in service today (Vrieling, A.,2006). In this paper, Landsat 8 TM data of the location Chittenden Peak (38°05'54.0"N 119°37'05.3"W) is used. Chittenden peak located in the Rocky Mountains with complicated terrain conditions of cliff, slope, river, vegetation cover and valley. A series of pictures are picked at different time of the day and at different seasons, they are processed using CC and SCS methods mentioned above and the result is compared.

2. Review of Topographic Normalization methods

2.1. Basic approach

Raw digital values (DVs) from the satellite optical systems cannot be directly used for geographical measurements and further studies. The raw data is affected by the atmospheric and topographic interferences. The atmospheric and BRDF correction approach are relatively well developed (Li, 2010). This paper mainly focus on the topographic correction. The model to obtain true reflectance from sensor radiance can be expressed as:

$$\rho_s = \frac{K\pi(\frac{L_{TOA} - L_0}{\tau_{uw}})}{E_0^{'}\cos\theta_z\tau_{dw} + E_h^{dif}} \quad (1)$$

In the equation, K is the correction factor of the annual variations of earth-sun distance. τ_{uw} is the path atmospheric transmittances of the upwelling (ground surface–sensor path) and τ_{dw} is the downwelling (sun–ground surface path) All other terms are defined in Table 5 in the appendix.

Topographic correction would affect the denominator term due to the illumination conditions of the sun and the terrain conditions. There are generally two approach or the topographic correction, the first approach does not require a DEM input such as the SCS method since the surface vegetation would change the terrain elevation. The reflectance is assumed to increase or decrease proportionally thus the topographic effect will be cancelled. (Colby, J. 1991; Short, N. 1982). This approach assumes that there is no diffusion irradiance. (Conese, C.,1993). This method also causes loss of spectral resolution. The second approach is to implement DEM data, the DEM data is required to compute the incident angle (i_t) which is the angle between ground normal and the sunlight. The modeling illumination condition configuration can be defined as following:

$$\cos(i_t) = \cos(\theta_s)\cos(\theta_t) + \sin(\theta_s)\sin(\theta_t)\cos(\varphi_s - \varphi_t) \quad (2)$$

All terms are defined table 5 in appendix. Figure 2 is a Schematic diagram of the configuration setup.

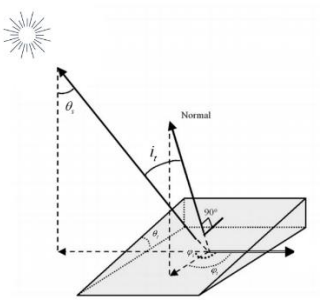

fig. 2 Schematic diagram of the configuration

2.2. C correction method

C correction method is based on a widely used model of simple cosine correction. Simple cosine correction is proposed by Teillet in 1982. This method starts out with the ratio between the total irradiance onto sloping terrain(E) and the total irradiance of the horizontal surface (E_h)

$$R = \frac{E}{E_h} = f_s \frac{\cos(i_t)}{\cos(\theta_s)} + (1 - f_s)F_d + F_t\rho_{adj} \quad (3)$$

Where f_s is the fraction of direct transmittance in the solar direction to the total transmission in the solar direction.

$$f_s = \frac{t_s}{T_s} \quad (4)$$

F_d is the factor for diffuse radiation, which is defined as:

$$F_d = V_d\left[1 + f_s \sin^3(\frac{\theta_t}{2})\right]\left[1 + f_s \cos^2(i_t)\sin^3(\theta_s)\right] \quad (5)$$

$$V_d = \frac{\left[1 + \cos(\theta_t)\right]}{2} \quad (6)$$

F_t is the nearby terrain radiation as:

$$F_t = V_t\left[1 + \sin^2(\frac{\theta_s}{2})\right]\left[\left|\cos\Delta\right|\right] \quad (7)$$

$$V_t = 1 - V_d \quad (8)$$

Δ is the azimuth of the inclined surface with respect to that of sun(lqbal,1983). R include direct irradiance (R^{dir}) and diffuse irradiance (R^{dif}). We got equation:

$$(R - a_t)S(1 - S\rho_m)\bar{\rho}^2 + \left[a_t + \rho_m(1 - a_t)S\right]\bar{\rho} - \rho_m = 0 \quad (9)$$

A_t is the total albedo of black sky albedo and white sky albedo. $\bar{\rho}$ is the bi-hemispherical factor. Equation for calculate a_t is listed in appendix. After substituted all terms in equation 3. The solution becomes

$$\rho_{lt} = \frac{\rho_m}{R + (1 - R)S\rho_m} \quad (10)$$

ρ_{lt} is the terrain irradiance corrected Lambertian surface reflectance factor. When the diffuse radiation is small, it can be ignored from the surrounding terrain and atmosphere. The horizontal surface reflectance can be simplified as:

$$\rho_{lt} = \rho_m \frac{\cos(\theta_s)}{\cos(i_t)} \quad (11)$$

This equation is the well known the simple cosine correction. However, when applying this model, several author state that this method have overcorrected the image, especially in areas of small incidence angle (Duguay, 1992; Meyer, 1993). This is caused by that the diffuse radiation has been ignored. To address and improve this problem, C-correction method is introduced. In this method, a regression model between $\cos(i_t)$ and ρ_m is implemented. The regression model is:

$$\rho_m = a\cos(i_t) + b \quad (12)$$

a is the slope of the regression line for the specific band, and b is the constant of the entire image. The corrected reflectivity is thus expressed as:

$$\rho_{CC} = \frac{\cos(\theta_s) + C}{\cos(i_t) + C} \quad (13)$$

C is the ratio between b and a (b/a). This has been proven to have a better-behaved correction for terrain than the cosine method (Soenen, 2005; Wu 2004). This method has

been proved to be successful in operational setting.

2.3 Sun-Canopy-Sensor correction method

Sun-Canopy-Sensor correction method is introduced by Gu Degui at 1998. This method uses the interaction between solar radiation and canopy elements as affected by the variation of terrain slopes and aspect. A geometrical presentation is shown in figure 3.

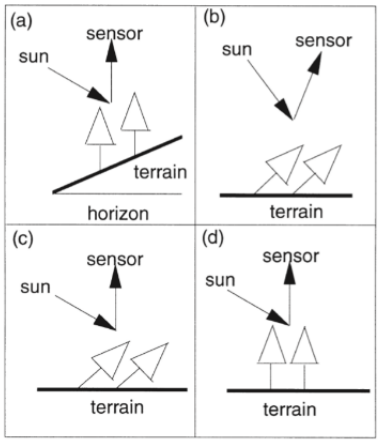

fig. 3 geometrical presentation of Sun-terrain-Sensor geometry correction model: a) forest canopy of the sloped terrain; b) terrain rotated to horizontal; c) after compensation based on photometric functions; d) forest canopy on flat terrain (Gu,1998)

The SCS method with the reflected radiance of the Sun-terrain-sensor(STS) geometry which is expressed as:

$$L=\rho E f(G)\cos\frac{i_t}{\pi} \quad (14)$$

Where E is the solar irradiance at earth surface. The STS model assumes that the interaction of light with a natural surface is determined by the geometry of light source and slopes. However, for land with vegetation cover, the light is scattered, transmitted and absorbed by the tree canopy. Since trees usually grow straight up toward sky no matter that slope is under it. So, the interaction is generally affected by the topography. The only effect of the topographic effect is the mutual interaction of light among tree canopy. This will result in more tree canopy exposed to the sun in the Sun-facing slop than the slopes facing away from the slope. By measuring the collective radiance from vegetations within the instantaneous field of view (IFOV) we can get the canopy's sunlit area and normalized it to remove the topographic effect. The geometry is shown in figure 4.

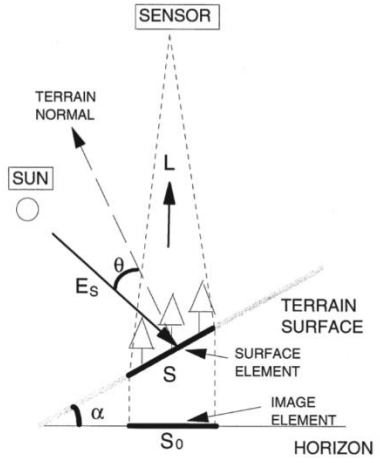

fig. 4 Geometry of the SCS correction method (Gu, 1998)

Since forest canopy is affected by many parameters such as stand type, seral stages and tree density, approximation formulations made to simplify the models. The total solar radiance energy(ε) is can be expressed as:

$$\varepsilon = ES\cos(i_t) \quad (15)$$

S is the area of the pixel on the slope. We set I as the average irradiance on the sunlit part of the canopy. The total area is

$$A=\frac{\varepsilon}{I} \quad (16)$$

The Area can thus be normalized to a horizontal terrain:

$$\frac{A}{A_0}=\frac{ES\cos i_t I_0}{ES_0\cos i_{t,0} I} \quad (17)$$

Term with subscript zero is the parameters on a horizontal terrain. Since the canopy is largely independent from the terrain, so we have relationship of $I = I_0$ and $S_0=S*\cos(\theta_t)$.

equation 17 can be simplifies as:

$$\frac{A}{A_0} = \frac{\cos(i_t)}{\cos(\theta_t)\cos(i_t)} \quad (18)$$

Since the LandSat TM sensor have a nadir view, the total radiance from the sunlit part of the canopy is proportional to the area. So the sensor radiance an be derived as:

When the surface is Lambertian (uniform bi-directional surface) the correction model of the surface correction as:

$$L_{TOA} = L_0 + \frac{\rho_m E_h T_v}{(1 - S\rho_m)\pi} \quad (19)$$

In this equation, L_{TOA} stand for the Radiance received by the sensor. L_0 is the path radiance. P_m is the atmospherically corrected Lambertian reflectance. Other terms are specified in Table 5.

$$L_{TOA} = L_0 \frac{\cos i_t}{\cos\theta_t \cos i_t} \quad (20)$$

Tree parameters used in simulating the forest Canopies is listed in table 2 in appendix.

2.4 Physics-based correction method

However, when the surface is non-Lambertian, things become more complicated since it describes the reflectance behavior at all possible angles of incidence, combined with all possible angles of reflection (Hu, 1999; Vermote 1996). The model to of the real reflectance of a non-uniform surface from sensor radiance maybe expressed as:

$$L_{TOA} = L_0 + \frac{1}{\pi} E'_0 \cos(\theta_S) \left(\begin{array}{l} t_V t_S \rho_S(\theta_S, \theta_V, \delta\varphi) + t_V t_d(\theta_S)\overline{\rho} + t_S t_d(\theta_V)\overline{\rho'} + \\ t_d(\theta_S) t_d(\theta_V)\overline{\overline{\rho}} + \dfrac{[t_V + t_d(\theta_V)][t_S + t_d(\theta_S)] S\left(\overline{\overline{\rho}}\right)^2}{1 - S\overline{\overline{\rho}}} \end{array} \right)$$

(21) (Li.f, 2012)

3. Study area and data processing

To get the best result of the study, locations are picked in the mountainous areas where shading variation is significant. Two study areas have been used in this research to represent the variation in various terrain. The first area located in the Australian Apls in the state of Victoria, this location has been picked as study area in Li' paper (Li.f, 2012). This paper will try to reproduce the result. The second location is in the Rocky Mountains, California, United states. The exact coordinate of the two locations are listed in Table 1. Both locations have gully in between the ridge and heavily shaded.

For testing the performance of algorithms at different solar angles and vegetation cover at different time of the year, four set of Landsat 8 images are obtained from earth explorer for location two. Detailed information of the five Landsat scenes are listed in Table 2.

Table 1.

Location number	Location	Longitude	Latitude
1	Victoria Alps	148.000 E	37.000 S
2	Rocky Mountains	119.617 W	38.099 N

Table 2

Number	date	Path	Row	Scene center solar position		
				Solar zenith	solar azimuth	solar distance
A	12/22/2019	91	85	30.697502	74.793022	0.983658
B	1/13/2019	42	34	62.69281	156.055908	0.983523
C	4/3/2020	42	34	48.725552	148.153854	0.991754
D	25/8/2019	42	34	32.811874	139.353302	1.1515

The topographic information in obtained by government released GIS data and digital elevation models (DEM) by SRTM data base. The GIS and DEM figure of the two locations are shown in figure 5. The elevation data can be extract from the DEM image (Zhan et al., 2002), and then the gradient of the slope can be calculated from using arctangent of the elevation over the distance of the elevation.

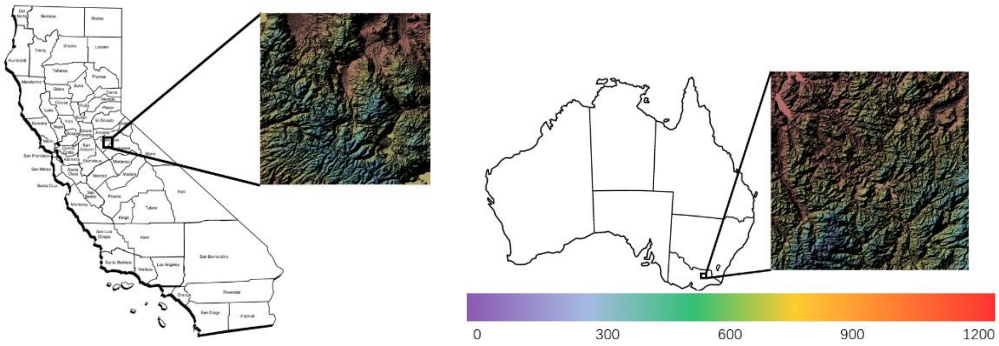

Figure 5. DSM data in the two study areas located on California and Australia Map

For each set of data, the image is processed with three different algorithms, (a) with natural color band composition, red color for band 4, green for band 3 and blue for band 2; (b) using the C-correction method to adjust the illumination factor of the shaded area. The C correlation factor is taken from Hantson's paper (Hantson,2011); (c) terrain corrected product from the SCS method. The result is evaluated by the image result the number of shaded pixels after the correction.

4. results

Both areas are chosen because they are typical regions with variety of landscape including tablelands, steep ravines, deeply cut river valleys and high relief with inaccessible, slopes covered by vegetations. The data is acquired from USGS Earth explorer website, all data is from Landsat 8 OLI/TIRS C1 Level-1 data base. The image is first processed with ArcGIS to composite the bands 2,3,4 and get the Standard RGB product. Then the data is processed with coordination system to match the image with GIS information to gather information about the topographic information for further analysis. All image is cropped to 1:200000 scale centered at the coordinate listed in table 1. Then the shadowed pixel number is recorded as a reference for evaluating the performance of each method.

For both algorisms, calculating the solar incidence angle on the surface is the first step of data processing. A build in function in ArcGIS can be used to achieve this goal. For C correction method, a regression coefficient is needed. As suggested by multiple authors, the regression coefficient should be acquired for individual locations for the best performance, however with the limited resources, this project used the same coefficient suggested by Li in her paper (Li fq, 2012) which works well for mountainous terrain. As for the SCS method, a standard tree canopy model is used, as for the main vegetation in Rocky Mountain area selected in this paper is redwood tree, we

select the cone-shaped tree parameter for simulating the forest canopies. The value of the simulation is listed in table 3.

Table 3 Tree Parameters of the Simulated Forest Canopies

Cone-shaped crown diameter	15m
Cone-shaped crown height	45m
Height of crown base to ground	28m
Reflectivity of tree crown	40%
Reflectivity of ground	40%
Distribution of trees	Random

Figure 5 present the image of the selected area before and after the correction using C correction and SCS correction. It's clear that the terrain shading at the hill scope scale has been reduced for both methods. As for the example of column (b) which is data of the Rocky Mountains collected at Jan,13 2019 has a larger solar zenith angle of 62.692810. It's is taken at time of California winter, so all the mountain tops are snow covered, the location of deep shallow has been lacking details. The shadow decrease as the solar zenith angle decrease, and there are fewer deep shadows in the other three scenes which have a much smaller solar zenith angle.

From the direct observance, a think fog like mask is covered above the image after processing. This is because that the atmospheric effect is enlarged by the correction method, several authors have suggested that an atmospheric correction should be done before the topographic correction. This result has proved that this process is necessary before the topographic correction.

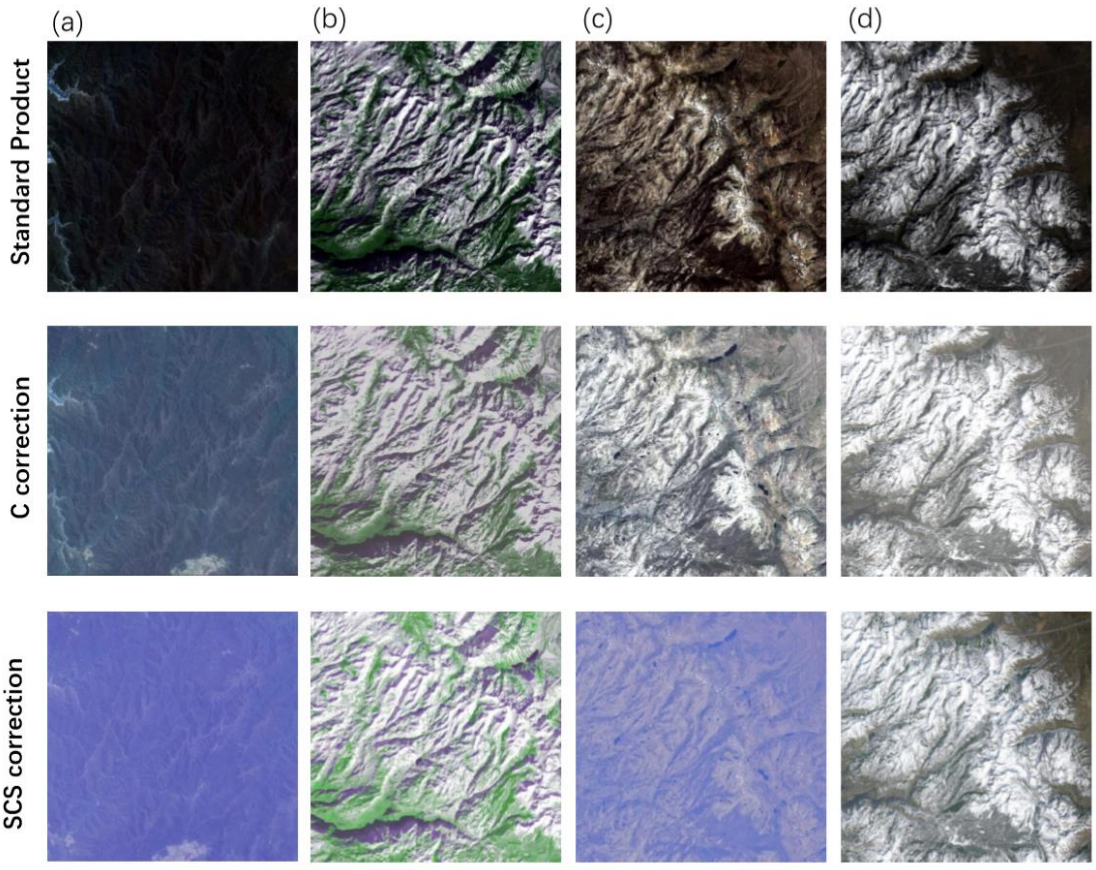

Figure 5. Nuture color composite image before and after correction

From the direct observance, a think fog like mask is covered above the image after processing. This is because that the atmospheric effect is enlarged by the correction method, several authors have suggested that an atmospheric correction should be done before the topographic correction. This result has proved that this process is necessary before the topographic correction.

The number of the shaded pixel is counted after the correction process and compared to the shadowed pixels before the process. The result is shown in table 4

Table 4 shaded pixel percentage relative to entire image

row	RGB	C-correction	percentage improvement	SCS	percentage improvement
a	1.29%	0.31%	0.758	0.35%	0.725
b	3.86%	1.08%	0.72	0.87%	0.775
c	1.96%	0.39%	0.801	0.27%	0.862
d	1.21%	0.35%	0.711	0.35%	0.716

As shown in the table, both methods have shown significant improvement on the shaded pixels of over 70 percent. The are some variations depending on the landcover and solar angle, but the overall performance is satisfying.

5. Conclusion

Based on data assessed by this paper, both methods have shown a great potential in correcting the geographic effects, C correction method generally shows better stability of result under different weather, landcover and seasonal conditions. However, acquiring the regression coefficient for different kind of land situations is an exhausting work requiring both in-situ measurements and remote sensing data to achieve the best result. On the other hand, physics-based method and the SCS method assume a vegetation model to acquire the parameters needed in the model. Although some authors concludes that SCS method didn't work well in their research, this method have achieved a decent result in data analyzed in this paper.

This paper is still lack of proper process of atmospheric correction, C-correction parameters and the sample number is not enough to draw a solid conclusion of which method is the best performing one. But as for the scenarios analyzed in this essay, both methods have shown a noticeable improvement.

Appendix

Table 5. Main symbols used in the paper.

θ_S	solar zenith angle
φ_S	solar azimuth angle
θ_V	sensor view zenith angle
φ_V	sensor view azimuth angle
θ_t	slope angle
φ_t	aspect angle of the slope
i_t	incident zenith angles between the sun and view directions and surface normal
φ_i	azimuth angle for incident direction in the slope

	geometry
e_t	exiting zenith angles between the sun and view directions and surface normal.
φ_e	azimuth angle for exiting direction in the slope geometry
t_S	direct transmittance in the solar direction
t_V	direct transmittance in the view direction
$t_d(\theta_S)$	diffuse transmittance in the solar direction
$t_d(\theta_V)$	diffuse transmittance in the view direction
S	the atmospheric albedo
T_S	total transmittance in the solar direction
T_V	total transmittance in the view direction
L_0	path radiance
E'_0	Solar exoatmospheric irradiance (earth-sun distance adjusted).
ρ_S	the surface reflectance (the BRF or bi-directional reflectance factor which is π times the BRDF)
ρ_{adj}	average reflectance of adjacent objects
ρ_m	the atmospherically corrected Lambertian reflectance
E_h	total irradiance on a horizontal surface
$E_{h,dir}$	the direct component of irradiance on a horizontal surface
$E_{h,dif}$	the diffuse component of irradiance on a horizontal surface
E	total irradiance on an inclined surface
E_{dir}	direct component of irradiance on an inclined surface
E_{dif}	diffuse component of irradiance on an inclined surface

Reference

"A field goniometer system (FIGOS) for acquisition of hyperspectral BRDF data," IEEE Trans. Geosci. Remote Sensing, vol. 37, pp. 978–986, Mar. 1999.

Bell, A. (1987). A satellite eye on soil erosion. Ecos, 51, 14-17.

Colby, J. (1991). Topographic normalization in rugged terrain. Photogrammetric Engineering and Remote Sensing, 57(5), 531-537.

Conese, C., Gilabert, M., Maselli, F., & Bottai, L. (1993). Topographic normalization of TM scenes through the use of an atmospheric correction method and digital terrain models. Photogrammetric Engineering & Remote Sensing, 59(12), 1745-1753.

David Riano. (2003) Assessment of Different Topographic Correctionsin Landsat-TM Data for Mapping Vegetation Types. IEEE transactions on geoscience and remote

sensing, vol. 41, no. 5, May 2003

Duguay, C., & Ledrew, E. (1992). Estimating surface reflectance and albedo from Landsat-5 Thematic Mapper over rugged terrain. Photogrammetric Engineering & Remote Sensing, 58(5), 551-558.

Dymond, J. R., Shepherd, J. D., & Qi, J. (2001). A simple physical model of vegetation reflectance for standardising optical satellite imagery. Remote Sensing of Environment, 77, 230–239.

Hantson, Stijn, & Chuvieco, Emilio. (2011). Evaluation of different topographic correction methods for Landsat imagery. International Journal of Applied Earth Observations and Geoinformation, 13(5), 691-700.

Hu, B., Lucht, W., & Strahler, A. (1999). The interrelationship of atmospheric correction of reflectances and surface BRDF retrieval - A sensitivity study. IEEE Transactions on Geoscience and Remote Sensing, 37(2), 724-738.

Ireland, H.A., Sharpe, C.F. and Eargle, D.H. 1939: Principles of gully erosion in the piedmont of South Carolina. Washington DC: US Department of Agriculture, Technical Bulletin 633.

Iqbal, M. (1983). An introduction to solar radiation (pp. 390). New York: Academic.

Kaufman, Y. J., and Sendra, C., 1 988, Algorithm for automatic atmospheric corrections to visible and near-IR satellite imagery, International Journal of Remote Sensing, 9, 1 357-1 381.

Li, F., Jupp, D., Thankappan, M., Lymburner, L., Mueller, N., Lewis, A., & Held, A. (2012). A physics-based atmospheric and BRDF correction for Landsat data over mountainous terrain. Remote Sensing of Environment, 124, 756-770.

Li, X., Strahler, A. H., & Woodcock, C. E. (1995). A hybrid geometric optical radiative transfer approach for modeling albedo and directional reflectance of discontinuous canopies. IEEE Transactions on Geoscience and Remote Sensing, 33, 466–480.

Liang, S. (2004). Quantitative Remote Sensing of Land Surface. : Wiley-Interscience 534 pp.

Meyer, Peter, Itten, Klaus I, Kellenberger, Tobias, Sandmeier, Stefan, & Sandmeier, Ruth. (1993). Radiometric corrections of topographically induced effects on Landsat TM data in an alpine environment. ISPRS Journal of Photogrammetry and Remote Sensing, 48(4), 17-28.

Richter, R. (1997). Correction of atmospheric and topographic effects for high-spatial-resolution satellite imagery. Proceedings of SPIE - The International Society for Optical Engineering, 3071, 216-224.

Richter R. (2009). Comparison of Topographic Correction Methods. Remote Sens. 2009, 1, 184-196; doi:10.3390/rs1030184

Schaaf, C., Gao, Strahler, Lucht, Li, Tsang, . . . Hu. (2002). First operational BRDF, albedo nadir reflectance products from MODIS. Remote Sensing of Environment, 83(1-2), 135-148.

Short, N. (1982). The LANDSAT tutorial workbook: Basics of satellite remote sensing. Feb 1982.

Soenen, S., Peddle, D., & Coburn, C. (2005). SCS C: A modified Sun-canopy-sensor topographic correction in forested terrain. IEEE Transactions on Geoscience and Remote Sensing, 43(9), 2148-2159.

Tricart, J. and Cailleux, A. 1972: Introduction to climatic geomorphology. London: Longman.

Vrieling, A. (2006). Satellite remote sensing for water erosion assessment: A review. Catena, 65(1), 2-18.

Vermote, E., Saleous, N. El, Justice, C. O., Kaufman, Y. J., Privette, J., Remer, L., et al. (1997). Atmospheric correction of visible to middle-infrared EOS-MODIS data over land surfaces: Background, operational algorithm and validation. Journal of Geophysical Research, 102(D14),

17131–17141.

Wu, X., Furby, S., & Wallace, J. F. (2004, October). An approach for terrain illumination correction. In The 12th Australasian remote sensing and photogrammetry conference proceedings, Fremantle, Western Australia (pp. 18-22).

X. Zhan, R.A. Sohlberg, J.R.G. Townshend, C. DiMiceli, M.L. Carroll, J.C. Eastman, M.C. Hansen, R.S. DeFries. RSE, 83 (2002), pp. 336-350